Optics Communications 315 (2014) 69–73

Contents lists available at ScienceDirect

Optics Communications

journal homepage: www.elsevier.com/locate/optcom

A development of two-dimensional birefringence distribution measurement system with a sampling rate of 1.3 MHz

Takashi Onuma [a,b,*], Yukitoshi Otani [a]

[a] Center for Optical Research & Education (CORE), Utsunomiya University, Utsunomiya-city, Tochigi 321-8585, Japan
[b] Photron Limited, Chiyoda, Tokyo 102-0071, Japan

ARTICLE INFO

Article history:
Received 11 September 2013
Received in revised form
25 October 2013
Accepted 29 October 2013
Available online 11 November 2013

Keywords:
Polarization
Birefringence
Measurement

ABSTRACT

A two-dimensional birefringence distribution measurement system with a sampling rate of 1.3 MHz is proposed. A polarization image sensor is developed as core device of the system. It is composed of a pixelated polarizer array made from photonic crystal and a parallel read out circuit with a multi-channel analog to digital converter specialized for two-dimensional polarization detection. By applying phase shifting algorism with circularly-polarized incident light, birefringence phase difference and azimuthal angle can be measured. The performance of the system is demonstrated experimentally by measuring actual birefringence distribution and polarization device such as Babinet–Soleil compensator.

1. Introduction

High-speed image sensors are used to capture transient phenomena that occur in a short period of time. The required time resolution varies according to the phenomena, but a sub-microsecond time range is useful in various applications such as impact test. Until now, although it has been applying to various applications, there are not so much reports concerning polarization applications. The phenomenon of polarization is utilized in various research fields, such as birefringence measurements, film thickness analysis, and surface roughness inspection. Furthermore, various techniques featuring rotating polarizer, photoelastic modulators and liquid crystal have been successfully demonstrated for polarization modulation [1–4], bringing further attention to the uses of polarization. Considering the recent direction in which technology is progressing, the importance of birefringence distribution measurements is increasing based on progress of material researches. Because currently established systems employ mechanical or electrical drives as polarization modulators, they require several photo-detection processes to measure polarization. In order to overcome this problem, a polarization image sensor has been proposed that can measure two-dimensional (2D) polarization by single photo-detection. The basic principle is the combination of a pixelated polarizer array with an image sensor. A pixelated polarizer array is composed of a thin film [5], a wire grid [6], element by electron beam lithography [7,8], and a photonic crystal [9]. The basic structural unit of these sensors is four polarizers, with their principal axes differing by 45°, attached to a 2×2 pixel matrix in order to obtain polarization information with spatial uniformity. Using these sensors, 2D polarization detection is possible at a sampling rate of around 30 Hz without any modulation. Other method has been proposed to increase sampling rate [10], but it has difficulty for practical use due to its special optical layout.

There, we propose a high-speed and 2D birefringence measurement system with a higher sampling rate of 1.3 MHz. A polarization image sensor is developed as core device of the system. Its design and fabrication incorporates a pixelated polarizer array and an image sensor with a parallel read out of a multi-channel analog to digital (A/D) converter specialized for 2D polarization detection. Actual performance of the developed system is experimentally demonstrated by applying it to impact test and measuring polarization devices.

2. Principle of birefringence measurement

The principle of the measurement system is shown in Fig. 1. The incident light becomes circular polarized light after passing through the polarizer (P) set with zero (0) degree angle and the quarter-wave plate at 45°. The circular polarized light then passes through the sample (X), having an unknown phase difference Δ and principal azimuthal angle φ, and further goes through the

* Corresponding author at: Takashi Onuma, Center for Optical Research & Education (CORE), Utsunomiya University, Utsunomiya-city, Toghigi 321-8585, Japan.
E-mail addresses: oonuma_t@opt.utsunomiya-u.ac.jp, oonuma@photron.co.jp (T. Onuma), otani@cc.utsunomiya-u.ac.jp (Y. Otani).

0030-4018/$ - see front matter © 2013 Elsevier B.V. All rights reserved.
http://dx.doi.org/10.1016/j.optcom.2013.10.086

linear polarizer as analyzer (A) with a fast axis orientation of 0°, 45°, 90° or 135°, and its light intensity distribution is finally measured by the photo detector.

We here assume S and S' as the Stokes parameter for the incident and outgoing light, respectively, that indicate the polarization state, and I_0 for the intensity of incident light. Then the Stokes parameter for the polarization state and conversion matrixes for each of the optical components are expressed as

$$S=\begin{bmatrix} S_0' \\ S_1' \\ S_2' \\ S_3' \end{bmatrix} \tag{1}$$

$$S'=\begin{bmatrix} S_0' \\ S_1' \\ S_2' \\ S_3' \end{bmatrix} \tag{2}$$

$$P_0=\frac{1}{2}\begin{bmatrix} 1 & 1 & 0 & 0 \\ 1 & 1 & 0 & 0 \\ 0 & 0 & 0 & 0 \\ 0 & 0 & 0 & 0 \end{bmatrix} \tag{3}$$

$$Q_{45}=\begin{bmatrix} 1 & 0 & 0 & 0 \\ 0 & 0 & 0 & -1 \\ 0 & 0 & 1 & 0 \\ 0 & 1 & 0 & 0 \end{bmatrix} \tag{4}$$

$$X_{\Delta,\varphi}=\begin{bmatrix} 1 & 0 & 0 & 0 \\ 0 & 1-(1-\cos\Delta)\sin^2 2\varphi & (1-\cos\Delta)\sin 2\varphi\cos 2\varphi & -\sin\Delta\sin 2\varphi \\ 0 & (1-\cos\Delta)\sin 2\varphi\cos 2\varphi & 1-(1-\cos\Delta)\cos^2 2\varphi & \sin\Delta\cos 2\varphi \\ 0 & \sin\Delta\sin 2\varphi & -\sin\Delta\cos 2\varphi & \cos\Delta \end{bmatrix} \tag{5}$$

$$A_{0,45,90,135}=\frac{1}{2}\begin{bmatrix} 1 & \cos 2\theta & \sin 2\theta & 0 \\ \cos 2\theta & \cos^2 2\theta & \sin 2\theta\cos 2\theta & 0 \\ \sin 2\theta & \sin 2\theta\cos 2\theta & \sin^2 2\theta & 0 \\ 0 & 0 & 0 & 0 \end{bmatrix} \tag{6}$$

The relation between the conversion matrixes of the optical components and the Stokes parameters for the incident and outgoing light is shown as

$$S'=A_{0,45,90,135}X_{\Delta,\varphi}Q_{45}P_0S \tag{7}$$

The outgoing light intensity I is S_0', and the incident light intensity I_0 is S_0. Here, intensity of the outgoing light I is obtained by using expressions (1)–(6) in the relation expression (7). The outgoing light intensity is expressed as

$$I=S_0'=\frac{1}{2}I_0(1-\sin\Delta\sin 2\varphi\cos 2\theta+\sin\Delta\cos 2\varphi\sin 2\theta) \tag{8}$$

We here assume the light intensity I_1, I_2, I_3 and I_4, when the fast axis orientation of the rotary analyzer on the outgoing light side is set to 0°, 45°, 90° and 135°, respectively, and apply the phase shifting method. Then the obtained incident light intensity I_0, the principal azimuthal angle of the sample φ and phase difference Δ are expressed as

$$I_0=\frac{I_1+I_2+I_3+I_4}{2} \tag{9}$$

$$\varphi=\frac{1}{2}\tan^{-1}\frac{(I_3-I_1)}{(I_2-I_4)} \tag{10}$$

$$\Delta=\sin^{-1}\frac{\sqrt{(I_3-I_1)^2+(I_2-I_4)^2}}{I_0} \tag{11}$$

Therefore, if the light intensity of the rotary analyzer (A) at each rotation angle is known, the incident light intensity, and phase difference Δ and principal azimuthal angle φ of the sample are calculated. The measurement dynamic range of Δ is quarter-wave of the wavelength of the light ($\pi/2$ rad) and that of φ is $\pm 90°$.

3. Development of high-speed polarization image sensor

Fig. 2 shows the difference in basic configuration between the general image sensor and the high-speed image sensor. In both sensors, each pixel has its own memory next to it. This mechanism allows the synchronism of exposure time across all pixels. In the general image sensor in Fig. 1(a), a read out circuit for the electric

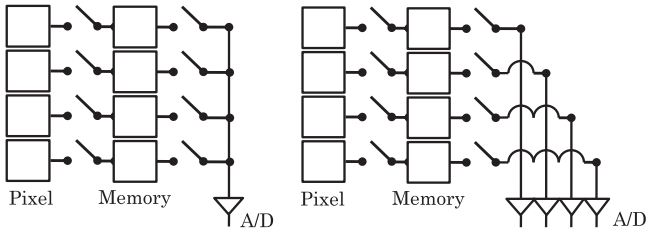

Fig. 2. (a) Basic configuration of the general image sensor. (b) Basic configuration of the high-speed image sensor.

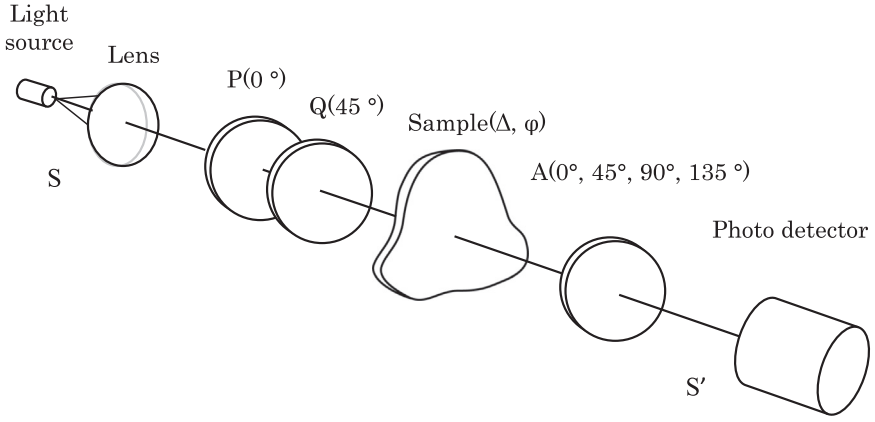

Fig. 1. Optical configuration.

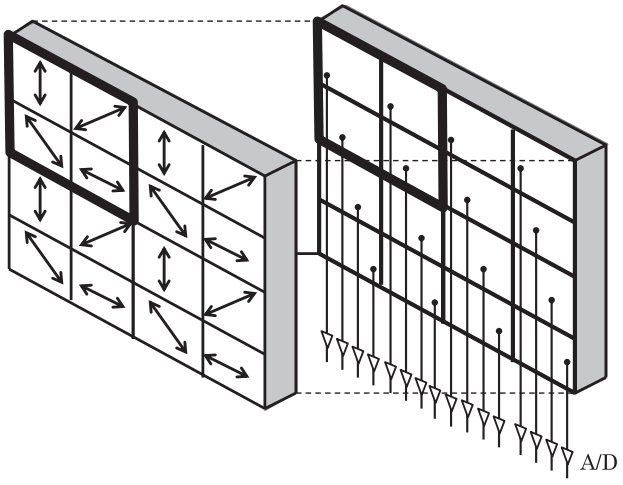

Fig. 3. Basic structural unit of the proposed sensor. The heavy line shows the four pixels needed to obtain one polarization datum. In order to obtain 2D polarization information, the matrix circuit with 16 A/D converters is directly connected to each pixel.

charges of the pixels is connected to a line of multiple pixels either vertically or horizontally. The electric charge of each pixel is read out sequentially through this line one by one. After that, they are digitized by a single A/D converter. Therefore, it is difficult to achieve a high sampling rate with such a 2D sensor. The basic configuration of the high-speed image sensor is shown in Fig. 1(b). Since multiple read out circuits are connected to multiple pixels, the electric charges of each pixel can be read-out in parallel. After that, they are digitized by multi-channel A/D converters while retaining synchronism. Therefore, this mechanism allows for the partial read out of the image sensor at a higher sampling rate.

Fig. 3 shows the basic structural unit of the 2D polarization image sensor composed of the parallel read out with multi-channel A/D converter. The pixilated polarizer array which is made from photonic crystal is bonded directly to the image sensor, making the optical system in this sensor resistant to vibration. Each polarizer corresponds to each pixel of the image sensor one by one. The size of each polarizer and pixel is $20 \times 20\ \mu m^2$. In the polarizer array groups of four neighboring polarizers (2×2) are set to have differing fast axis orientation at 0°, 45°, 90° and 135° in a clockwise arrangement. One polarization datum can be obtained by calculating detected light intensities from the four pixels of the image sensor. Consequently, the parallel read out circuit has to be arranged in a corresponding matrix. Moreover, in order to obtain 2D polarization information, 16 polarizers (4×4) are employed as unit structure. Thus, we designed 16 parallel read out circuits in a matrix in the image sensor, which are connected to each pixel with individual A/D converters. With this structure, 2D polarization information (2×2) can be obtained simultaneously. Through skipping of sequential read out process, this method allows for a shorter sampling time up to around 700 ns for the single read of one pixel. By combining various basic structural units with simultaneous processing systems, more pixels can be read at the same time.

Fig. 4 shows the internal structure of a polarization detecting system with a sampling rate of 1.3 MHz using the proposed sensor. Eight basic structural units are combined with a simultaneous processing system. Electric charges that represent 2D polarization information from eight units pass through a Multiplex circuit and are written to the memory. By repeating this process, the sensor records 2D information continuously. The maximum sampling rate of the system is 1.3 MHz with 32×4 pixels. By arraying this structure with a batch process, a 1024×1024 pixel sensor with a sampling rate of 5 kHz is possible.

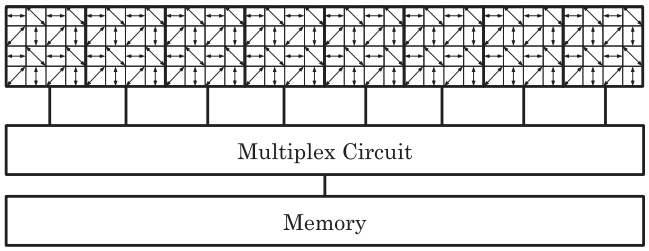

Fig. 4. Internal structure of a polarization detecting system with a sampling rate of 1.3 MHz.

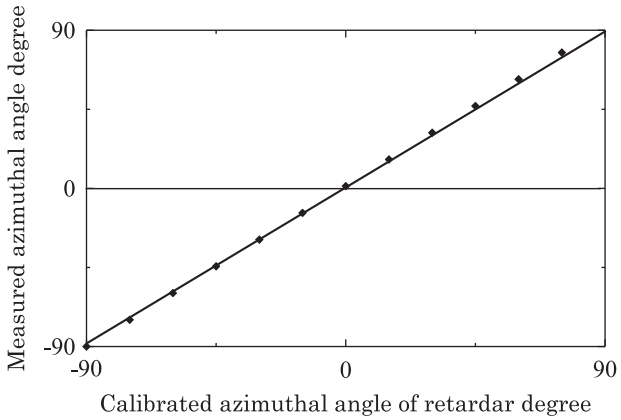

Fig. 5. Repeating accuracy of the azimuthal angle.

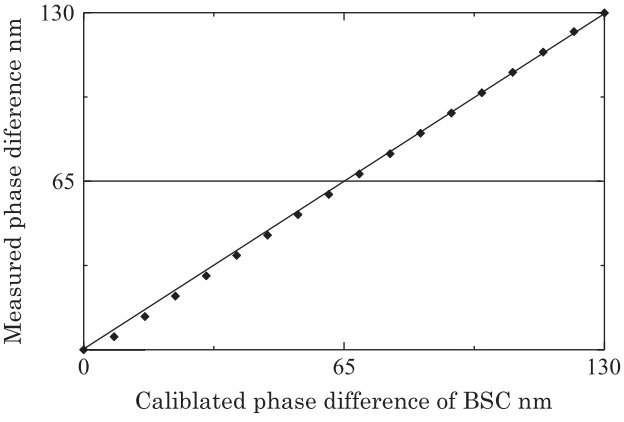

Fig. 6. Repeating accuracy of the birefringence retardation.

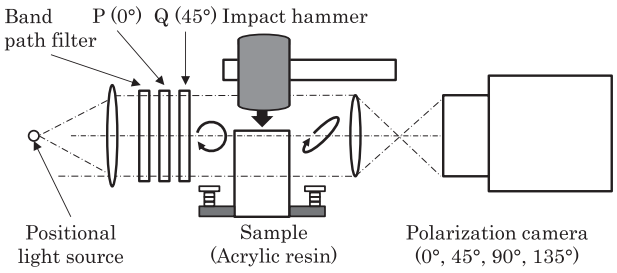

Fig. 7. Experimental setup.

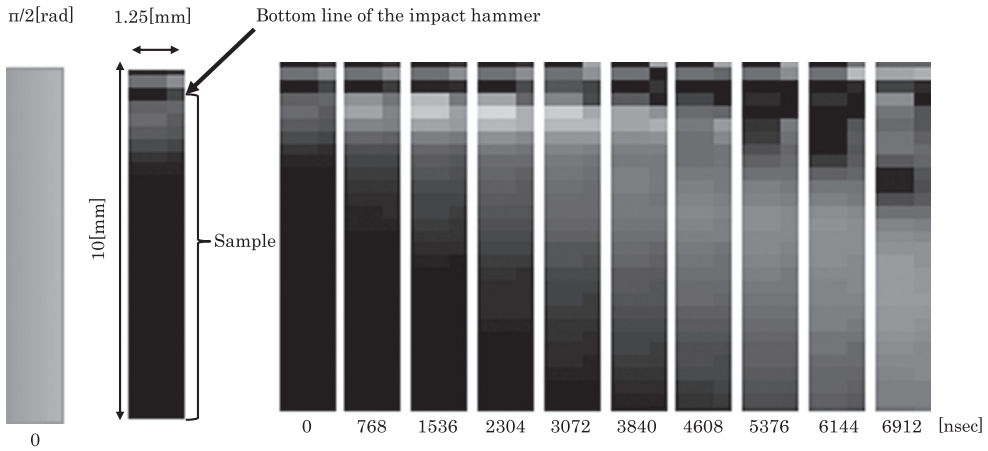

Fig. 8. Experimental results of time series images. Birefringent phase difference distribution at a sampling rate of 1.3 MHz with 32×4 pixels is seen. Measurement range of the phase retardation was 1/4 of the wavelength (520 ± 20 nm) as shown in 256 steps of the grayscale.

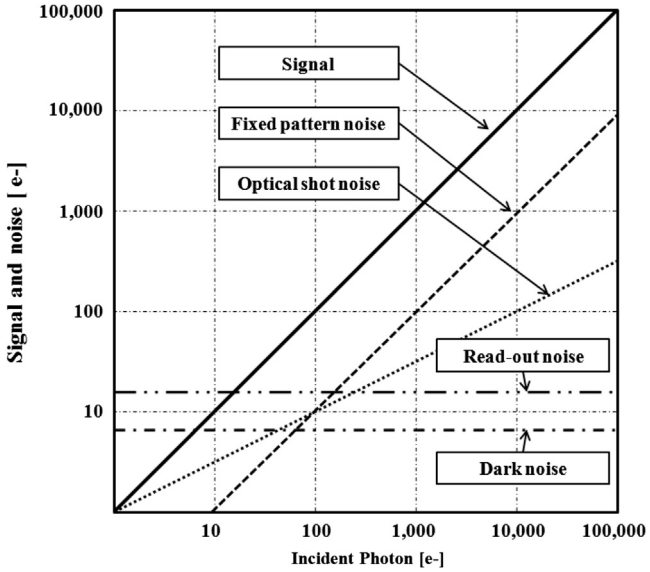

Fig. 9. Noise from the image sensor.

4. Validation of accuracy

4.1. Accuracy validation of azimuthal angle

We carried out an accuracy validation test of azimuthal angle using the optical system shown in Fig. 1. Measured value is shown by points and theoretical value shows solid line in Fig. 5 when the retarder, used as a sample, was rotated. The error range of this measurement result was $\pm 1.13^{\circ}$.

4.2. Accuracy validation of phase difference

Using the same setup as in the above, we made an accuracy validation test of phase difference. The measured result of phase difference being varied from 0 nm to 130 nm, by way of a Babinet–Soleil compensator, is shown in Fig. 6. With the above result, the error range of this measurement result was ± 1.28 nm.

5. Experimental setup and results

We confirmed the actual performance of the developed system by hitting a block of acrylic material with a hammer. The 2D distribution of the birefringent phase difference was dynamically measured. Fig. 7 shows the experimental setup. The hammer impacts the top center of the acrylic block from above. The collimated incident light with wavelength 520 ± 20 nm is circularly polarized using a polarizer P at 0° and a quarter-wave-plate Q at 45°. The circularly polarized light passes through the sample, with unknown phase difference Δ. After that the light intensity is measured with the polarization camera containing a high-speed polarization image sensor at a sampling rate of 1.3 MHz. The electric charges that represent the light intensities accumulated from each pixel are quantized by the multi-channel A/D converters and are stored in the memory of the camera. After that, we repeatedly applied a phase shift analysis process to the stored data to obtain time-serial images of birefringent phase difference.

Fig. 8 shows experimental result of time series images. The birefringent phase difference distribution in the acrylic resin is shown by grayscale divided into 256 steps of measurement dynamic range that is changed from black to white. When the

Table 1
Repeat accuracy of the proposed system by time averaging.

Average number frame	Repeat accuracy of phase difference (nm)	Repeat accuracy of azimuthal angle (deg)
1	0.481	1.117
10	0.195	0.392
100	0.086	0.145

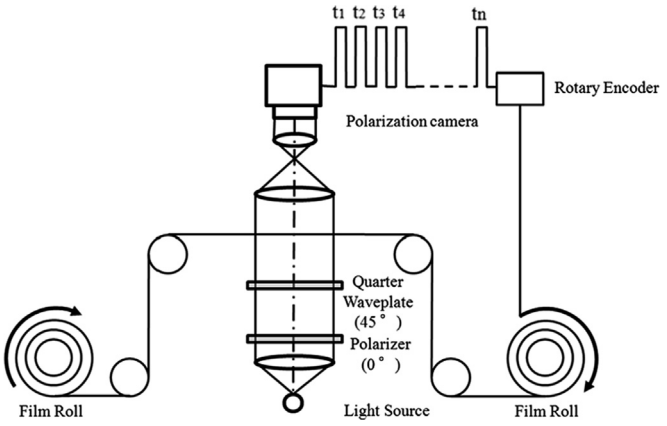

Fig. 10. Experimental setup of the birefringence mapping.

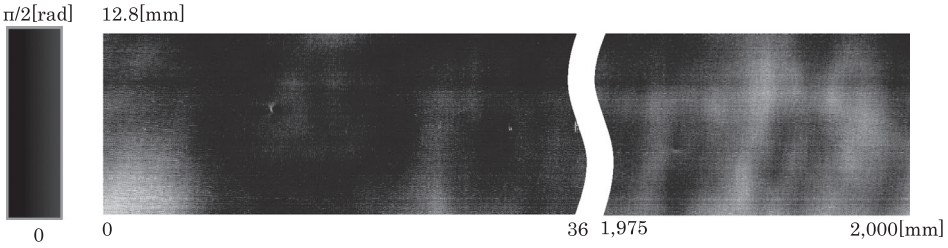

Fig. 11. Experimental result of birefringent phase difference distribution of transparent film.

measured phase difference Δ is increased over dynamic range of measurement expressed in Eq. (11), phase jump will be occurred. After $\pi/2$ rad, phase difference is shown by grayscale of opposite direction that is changed from white to black until π radian. This representation is repeated every π radian in resultant images.

Looking at the resultant images of the measurement, although measured phase difference seems to be increased over measurement dynamic range in the time around 2304 ns, we can clearly confirm that birefringence propagates from the impact point to deeper part of the material with sub-micro-second time resolution.

6. Accuracy improvement by time-frames

Since proposed system employs image sensor in order to measure intensity of the light, it is important to consider relation between signal and noise of the sensor. Image sensor is prone to have four different types of noises. They are optical shot noise, dark current noise, readout noise and fixed pattern noise. The relation between the incident light and output light with the photoelectric conversion efficiency of 100% is shown in Fig. 9. Read out noise can be canceled by measuring signal under the light interception condition. Error effect of the dark noise is much lower than that of others. Although, fixed pattern noise is increased in proportion to the light intensity, it can be corrected by measuring input–output characteristics of luminance transition by integrating sphere. However, since optical shot noise is occurred in random and increased in proportion to the light intensity, we assumed it makes a great effect on the repeat accuracy of the measurement result.

Averaging method is one of the approaches to reduce random noise. Since proposed system offers high sampling rate, utilize of data on time axis is effective. There, we evaluated the effect of time averaging by 1, 10, and 100 of the time frames using optical setting shown in Fig. 1 with no sample condition. Averaging is applied to detected light intensities of each pixel before applying phase shifting calculation. Table 1 shows the result of relation between average number and repeat accuracy of the phase difference and azimuthal angle calculated by expressions of (9)–(11). As a result, effectiveness of higher sampling rate for higher accuracy is confirmed by applying time averaging method.

7. Experiment of phase difference mapping

Recently, optical transparent films are mainly used in flat panel display such as LCD. Since these films control polarization status, in-plane uniformity of film's birefringence distribution is essential of it.

As an application example of developed system, birefringence distribution of the transparent film has been measured. Fig. 10 shows experimental setup. Polarization camera and light systems are set above and below the film. The film is mechanically transferred. Each image is synchronized with transferring film by each pulse from rotary encoder attached to the film role. Number of pixels of each image is 128×4 by arraying basic unit structure of the 2D polarization sensor. After taking images, all images are combined as one image. The result is shown in Fig. 11. Phase difference is shown by grayscale, and its distribution can be seen on entire measured area.

8. Conclusions

In conclusion, we have developed a two-dimensional birefringence measurement system with a sampling rate of 1.3 MHz. Proposed system is composed of polarization image sensor based on a pixelated polarizer array with a multi-channel A/D converter. The most unique feature of this system is the fast sampling rate. Actual performance of it is shown by using birefringence propagation in acrylic resin. With the conventional point measurement techniques, it is difficult to see and determine the direction of birefringence propagation. Also, with the conventional 2D birefringence measurement, sampling rate of sub-micro-second has not proposed yet. From these points, we believe, proposed system can be powerful tools in order to help and understand of unsolved phenomena such as impact fracture mechanism of the materials. Moreover, effectiveness of accuracy improvement by fast sampling rate is confirmed. We are expecting to improve further high accuracy by using time axis information. Lastly, phase difference map of transparent film is made as application example.

There are many dynamic 2D phenomena that feature an associated change in polarization, which in turn means there are many potential applications for this system and high-speed polarization sensor. Hence, we are expecting co-researchers in various specialized areas to make use of our sensor.

In future work, we will strive for an even faster sampling rate of polarization imaging. Moreover, from the point of practical application view, we aim to research and develop a more compact measurement system and the measurement method for high-order phase difference.

References

[1] M. Noguchi, T. Ishikawa, M. Ohno, S. Tachihara, Proc. SPIE 1720 (1992) 367.
[2] Y. Otani, T. Shimada, T. Yoshizawa, N. Umeda, Opt. Eng. 33 (1994) 1604.
[3] A.M. Glazer, J.G. Lewis, W. Kaminsky, Proc. R. Soc. London A 452 (1996) 2751.
[4] M.I. Shribak, R. Oldenbourg, Proc. SPIE 4819 (2002) 56.
[5] V. Gruev, J.V. Spiegel, N. Engheta, Opt. Express 18 (2010) 19292.
[6] J. Millerd, N. Brock, J. Hayes, M.N. Morris, M. Novak, J. Wyant, Proc. SPIE 5531 (2004) 301.
[7] H. Kikuta, K. Numata, M. Muto, K. Iwata, Polarization imaging camera with a form birefringent micro-retarder array, in: OSA Technical Digest Paper ThRR3, 2003.
[8] S. Yoneyama, H. Kikuta, K. Moriwaki, Opt. Eng. 45 (2006) 083604.
[9] L. Fabre, Y. Inoue, T. Aoki, S. Kawakami, Appl. Opt. 48 (2009) 1347.
[10] K. Oka, Y. Ohtsuka, Exp. Mech. (1993) 44.